Korean J. Chem. Eng., 35(10), 1969-1978 (2018)
DOI: 10.1007/s11814-018-0128-3

pISSN: 0256-1115
eISSN: 1975-7220

Rheo-kinetics of bovine serum albumin in catanionic surfactant systems

Osita Sunday Nnyigide and Kyu Hyun†

School of Chemical and Biomolecular Engineering, Pusan National University, Busan 46241, Korea
(*Received 28 May 2018 • accepted 18 July 2018*)

Abstract−The effects of catanionic surfactant systems consisting of mixtures of cationic cetyltrimethylamonium bromide (CTAB) and anionic sodium dodecyl sulfate (SDS) on the rheological properties and kinetics of bovine serum albumin (BSA) were investigated. The ionic strength of the solution was varied by using different mixing ratio of SDS and CTAB. Gelation curves observed in dynamic viscoelastic measurements were fitted with gelation kinetics models to describe the gelation under isothermal and non-isothermal conditions. Overall, the gelation of BSA in cationic-rich solutions was found to be more energetically favorable when compared with BSA solvated in anionic-rich solutions. Consequently, highest gel temperature (T_{gel}) and time (t_{gel}) were observed for anionic-rich solutions with SDS/CTAB molar ratio of 4.0 (i.e., SDS/CTAB=4.0), while lowest gel temperature and time were found for cationic-rich solutions with SDS/CTAB molar ratio of 0.25 (SDS/CTAB=0.25). BSA in equal molar ratio of the mixed surfactants (SDS/CTAB=1.0) showed a gel temperature and time in the halfway between the anionic and cationic-rich regions. Interestingly, under isothermal and non-isothermal conditions, BSA in equimolarly mixed and anionic-rich solutions showed a heat-dependent protective effect against thermal denaturation and gelation. The protective effect on BSA gelation in equimolar and anionic-rich solutions was diminished by increasing the catanionic concentration under non-isothermal conditions, while under isothermal conditions, protective effect on BSA gelation increased with catanionic concentration. On the other hand, cationic-rich solutions did not protect BSA from thermal denaturation and gelation, and therefore the gelation rate increased with catanionic concentration in all heating conditions examined.

Keywords: CTAB, SDS, Catanionic Surfactant, Bovine Serum Albumin (BSA), Rheology

INTRODUCTION

Bovine serum albumin (BSA), also known as Fraction V, is considered to be a universal bio-reagent in many applications [1,2]. As a model protein, a large amount of research work has been conducted on BSA protein owing to its lack of effect on many biochemical reactions, and its low cost, since large quantities of it can be readily purified from bovine blood, a byproduct of the cattle industry. BSA has the most widely reported binding sites, and is known to bind to various surfactants and biologically relevant substances [3-8]. The crystal structure of BSA reveals a heart-shaped structure with three domains of which each is divided into subdomain A and B [9]. The primary structure of BSA is composed of a sequence of 583 amino acid residues, and its secondary structure contains 67% alpha helix and 17 disulfide linkages [8,9]. The isoelectric point (IEP) of BSA is at pH 4.5-5.0; therefore, the protein is negatively charged at neutral pH.

Catanionic surfactant systems which display a large diversity of phases consist of oppositely charged ionic surfactants [10]. They have drawn much attention recently because of their rich bulk and interfacial properties [10,11]. The structure of catanionic surfactants is similar to that of zwitterionic surfactants, such as phospholipids; however, their polar head group is composed of two oppositely charged groups that are not covalently bonded unlike zwitterionic surfactants [10-12]. As opposed to protein solution in single anionic or cationic surfactants, the very strong synergism between oppositely charged cationic and anionic surfactants makes the formation of catanionic surfactant mixed aggregates in the bulk solution a more favorable process than binding to proteins [11]. The interactions of proteins with catanionic surfactants are scarcely reported in the literature and have rarely been investigated. This might be because most of the mixed catanionic surfactants form precipitates or become turbid at very low concentration, which limits the research of their interactions with proteins [11]. However, it is important to investigate their interactions because it is very often that proteins and surfactants are present in the same systems, especially in gel filtration chromatography for protein separation or purification [10,11].

In biopolymer solutions, the pH value and electrostatic charges are of crucial importance as they determine the colloidal behavior as phase separation, precipitation or complete miscibility [13,14]. When a protein-denaturant solution is heated above the protein denaturation temperature, which is typically >55 °C, the protein unfolds substantially and under continuous heating the unfolded protein aggregates to form a gel [1,16-19]. Initially upon heating, the onset of gelation or phase change is accompanied by sudden increase in solution viscosity. The protein gelation kinetics is governed mainly by two important steps: first, the unfolding or dissociation of the protein molecules induced by a chemical denaturant or heat, and second, the association and aggregation of denatured protein chains, which is achievable only in the presence of suitable environmental conditions [1]. In this manner, the protein progressively passes from the native state to a denatured and unfolded transition state, and

†To whom correspondence should be addressed.
E-mail: kyuhyun@pusan.ac.kr

then to an aggregate network that forms a soft gel, which eventually reaches the final rigid gel state [1,16-19]. The rate of denaturation or aggregation which is influenced by heat or chemical denaturants affects the texture and rigidity of the final gel formed. Thus, for various gel applications, the strength of the gels can be tuned by varying the denaturant concentration/composition and the heating method (i.e., isothermal/non-isothermal heating). The enhancement in the gel properties achieved under this condition has potential for many promising applications, such as catalysis, drug delivery, protein chromatography, tissue and cell surface engineering [20-22].

To investigate the structural changes that take place upon heating of a polymer solution, both rheology and differential scanning calorimetry (DSC) can provide information at physical and macroscopic levels, indicating changes associated with gelation or denaturation processes [23-32]. However, DSC measurement sometimes is not able to detect gelation temperature or time by providing required endothermic curve [32]. For this reason rheological properties measurement is usually preferred as a means of evaluating the gelation process and gel strength because it is able to provide accurate information as regards to gelation temperature or time of the sample solution [32]. For instance, a temperature ramp test provides information on the transition temperature from the solution state to the gel state in terms of the dramatic change in rheological properties as temperature increases [1,23]. Also, the degree of gelation, gel time, and sol-gel transition can be determined using a time sweep test rheological method [32]. Moreover, measurable material properties from rheological measurements such as the storage modulus (G′) can be fitted with reaction kinetic models to derive useful kinetic parameters, which can provide more insight into the gelling mechanism and for a potential substitution of one protein for another in food systems [24-27]. Thus, the measurements of the rheological properties are effective tools for monitoring the unfolding, aggregation/gelation, or stability of proteins.

The motivation for this study comes from our previous investigation where the gelation of BSA was markedly affected by the addition of SDS or CTAB. Consequently, we sought to use the mixture of SDS and CTAB to provide a wide range of chemistries and different combinations of physical and chemical cross-links/interactions, and thus, generating results with wide ranging applications. The objective of this study therefore was to characterize the effects of catanionic surfactants on BSA gelation temperature (T_{gel}) under non-isothermal heating and on BSA gelation time (t_{gel}) under isothermal heating at above the T_{gel} of BSA using rheological measurements. The gelation curves at constant temperatures observed in time sweep measurement, and at increasing temperature observed in temperature ramp test were fitted with reaction kinetic models.

EXPERIMENTAL PROCEDURE

1. Sample Preparation

BSA (product No A7906), SDS (product No L3771), CTAB (product No H9151) and Phosphate Buffered Saline, PBS (product No P5493) were purchased from Sigma-Aldrich. The supplied samples were used without further modification. PBS diluted ten times with distilled water was used as solvent. BSA was solvated in the diluted PBS and stirred for 1 hour at room temperature. Sample pH was adjusted to 7.0 using PBS. 5, 7 and 10 wt% BSA solutions were prepared and catanionic surfactant from 0.01-0.05 M were added to the solution. Each catanionic solution consisted of SDS/CTAB molar ratio of 0.25, 1 and 4. The chemical structures of SDS and CTAB are provided in Fig. 1.

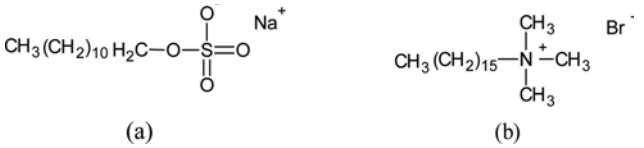

Fig. 1. Chemical structure of (a) the anionic surfactant, Sodium Dodecyl Sulphate (SDS) and (b) of the cationic surfactant, Cetyltrimethylammonium Bromide (CTAB).

2. Rheological Measurements

Rheological measurements were performed on an ARES-G2 (strain-controlled rheometer, TA Instruments, USA) using a concentric cylindrical geometry (40 mm diameter cup, 27.7 mm diameter bob) for time sweep tests, and parallel plate geometry (40 mm diameter) for temperature ramp tests. Silicon oil was placed around samples to prevent evaporation. Time sweep tests were carried out to monitor the evolution of gel structures at a frequency (ω) of 1 rad/s and a strain amplitude (γ_0) of 0.05 (linear viscoelastic regime) [1,29]. Temperature ramping was used to determine gel thermal properties at ω=1 rad/s, γ_0=0.05, 25-90 °C, and a heating rate of 0.5 °C/min.

RESULTS AND DISCUSSION

1. Non-isothermal Gelation of BSA/Catanionic Solution

The thermal properties of BSA/catanionic solutions were investigated by ramping temperature from 25-80 °C for BSA/catanionic solutions with SDS/CTAB=0.25 and 1.0, and from 25-90 °C for BSA/catanionic solutions with SDS/CTAB=4.0. The reason for choosing different temperature range was due to high gelation rate of BSA in cationic-rich solutions when compared with anionic-rich solutions. A low heating rate of 0.5 °C/min was used, which is recommended for investigating microstructural changes in non-isothermal gelation [1]. All measurements were carried out at low strain amplitude (γ_0=0.05) within the linear viscoelastic region to avoid sample breakdown [1,29]. A typical non-isothermal gelation process of the BSA/catanionic solution is shown in Fig. 2(a), and the rest are shown in supporting information Figs. S1-S3. The point of rapid increase in storage modulus (G′) was taken as the onset of phase change and gelation. By heating the BSA/catanionic solutions, the viscoelastic material functions dramatically changed due to protein denaturation which is a precursor to gelation. The interactions between denatured BSA chains resulted in aggregation and gelation of the protein-catanionic solutions [1,33-38]. At temperatures up to 52 °C for BSA/catanionic with SDS/CTAB=0.25 and 1.0; and up to 71 °C for BSA/catanionic with SDS/CTAB=4.0, the storage moduli appeared to be relatively independent of temperature (supporting information Fig. S1-S3). This is presumably because the denatured chains of BSA had insufficient energy to initiate aggregation. Migliori et al. and Chen et al. [39,40] likened this initial

increase in temperature without corresponding increase in moduli up to the onset of gelation to a kinetic effect caused by the temperature increase that tends to weaken the molecular structure of the biopolymer solution. However, at temperatures >55 °C for BSA/catanionic with SDS/CTAB=0.25 and 1.0; and >75 °C for BSA/catanionic with SDS/CTAB=4.0, positive dependence of storage moduli on temperature evolved, which indicated increased solution viscosity due to thermal denaturation and intermolecular aggregation [1,39,40]. Furthermore, this evolution of temperature-dependent storage moduli was found to depend on the concentration of the catanionic surfactant and the SDS/CTAB mixing ratio. On further heating, increased thermal denaturation enhanced BSA aggregation and gel formation, because as previously reported exposed hydrophobic sites are very unstable in aqueous environments [1]. The gelation temperature of BSA solutions containing different catanionic surfactant concentrations varied significantly and was found to depend on the SDS/CTAB mixing ratio. As can be seen in Fig. 2(a), the solutions easily showed elastic behavior (i.e., G′=G″) for a wide range of temperature, which made it difficult to accurately detect the gelation temperature (T_{gel}) by the cross-over of G′ and G″ curves. Therefore, T_{gel} was determined using a differential method [1] (supporting information Fig. S1(f)). The differential method is based on determination of the inflexion point or the turning point of G′ spectra. Plot of T_{gel} for 10 wt% BSA versus catanionic surfactant concentration is shown in Fig. 2(b). The lowest T_{gel} was observed for BSA in cationic-rich solutions, while highest T_{gel} was found for BSA in anionic-rich solutions which is in good agreement with isothermal gelation discussed later.

2. Effects of BSA and Catanionic Concentration on the T_{gel} of BSA/Catanionic Solutions

The effects of BSA and catanionic concentration on the T_{gel} were investigated using BSA concentrations of 5 and 7 wt%, in addition to 10 wt% (discussed above), and catanionic concentrations of 0.01-0.05 M. The G′ curves for 7 and 5 wt% are shown in supporting information Figs. S2 and S3. The gel temperature (T_{gel}) was found to decrease slightly with increase in BSA concentration throughout the catanionic concentration range examined (Fig. 3). This is in agreement with the observations in time sweep test (discussed later), and was attributed to more protein-protein interactions on increasing BSA concentration. In the case of 7 and 10 wt% BSA

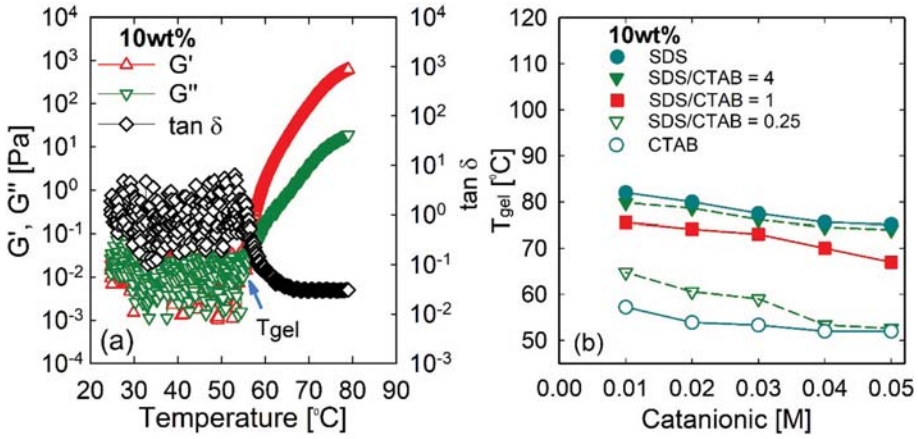

Fig. 2. (a) Temperature ramp test for 10 wt% BSA solution with 0.05 M catanionic surfactant (SDS/CTAB=0.25) with frequency of ω=1 rad/s, strain amplitude γ=0.05, heating rate=0.5 °C/min. (b) Gel temperature for 10 wt% BSA solution with 0.01-0.05 M catanionic surfactant and various SDS/CTAB mixing ratio.

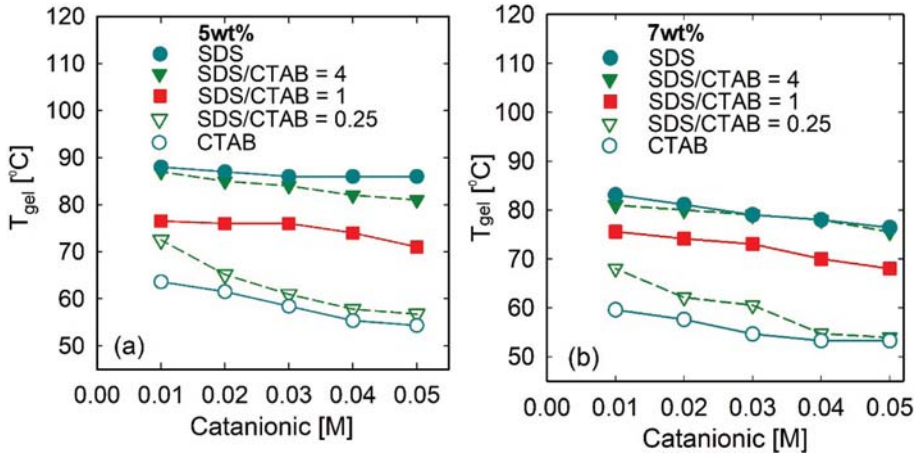

Fig. 3. (a)-(b) Gel temperature for 5 and 7 wt% BSA solutions with 0.01-0.05 M catanionic surfactant and various SDS/CTAB mixing ratio, with frequency of ω=1 rad/s, strain amplitude γ=0.05, heating rate=0.5 °C/min.

with SDS/CATB=1, it was difficult to distinguish between their T_{gel} (supporting information Figs. S1 and S2). In addition, the T_{gel} was found to decrease with increase in catanionic concentration at all BSA concentration range and SDS/CTAB mixing ratio examined. This appeared to suggest that the rate of protein denaturation also increased with catanionic concentration. Comparatively, the T_{gel} of 5, 7 and 10 wt% BSA decreased in the order of 0.25<1<4 of SDS/CTAB mixing ratio. Overall, a faster rate of gelation or lower T_{gel} was observed for cationic-rich solutions than the equimolarly mixed or anionic-rich solutions.

3. Non-isothermal Kinetic Modelling of BSA/Catanionic Solutions

The gelling of BSA/catanionic solutions can be modelled using the concept of the minimum energy required for solutions to gel (i.e., activation energy) and the dependence of gelation rate on reactant concentrations (i.e., order of reaction). We carried out non-isothermal kinetic modelling based on our experimental data, as has been previously described [32,41-44]. For an n^{th} order reaction the reaction rate is described by:

$$-\frac{dC}{dt} = kC^n \tag{1}$$

where C is concentration, t is time and k is the reaction rate constant. The temperature dependency of reaction rate constant k is well represented by the Arrhenius relationship:

$$k = k_0 \exp\left(-\frac{E_a}{RT}\right) \tag{2}$$

Combining Eqs. (1) and (2) and taking a logarithmic transformation yields:

$$\ln\left(-\frac{1}{C^n}\frac{dC}{dt}\right) = \ln k_0 - \left(\frac{E_a}{R}\right)\left(\frac{1}{T}\right) \tag{3}$$

The kinetic parameters, E_a and k_0 are the activation energy and the pre-exponential or frequency factor, and these are estimated using Arrhenius plots of Eq. (3).

During non-isothermal gelation, the protein unfolds, aggregates, and then cross-links to form a gel. Gelation occurred at relatively high temperature (70-85 °C for BSA/catanionic with SDS/CTAB= 4 and 53-75 °C for BSA/catanionic with SDS/CTAB=0.25 and 1, respectively, see Fig. 2(b) and Fig. 3) and this was in part responsible for the rigidity of the gel formed. The kinetic Eq. (3) can be converted to Eq. (4) in terms of rheological parameters (G′ and dG′) instead of reactant concentration (C) and change in concentration (dC), respectively. This can be explained by the rubber theory of elasticity [43-45]. The negative sign of Eq. (3) is replaced by a positive sign because G′ increases at gelation (positive dG′). Eq. (3) can be converted to the linear form below

$$\ln\left(\frac{1}{G'^n}\frac{dG'}{dt}\right) = \ln k_0 - \left(\frac{E_a}{R}\right)\left(\frac{1}{T}\right) \tag{4}$$

Using Eq. (4) the derivatives of experimental data can be calculated by the following methods: (i) graphical differentiation [41], (ii) polynomial curve fitting and differentiation of the fitted equation [32], and (iii) numerical differentiation as described by Rhim et al. [42]. In this report, we used linear regression analysis to determine the order of reaction (n) and the activation energy (E_a) after differentiating experimental data numerically.

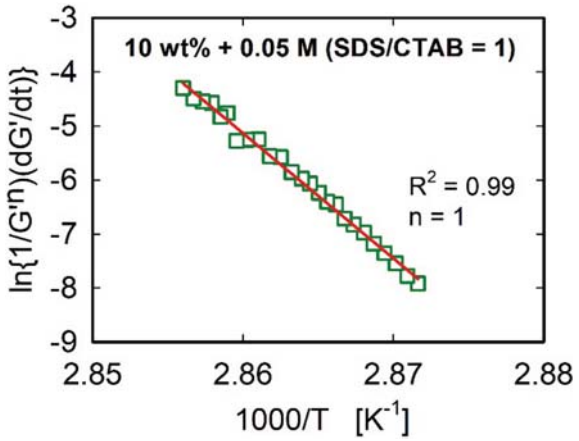

Fig. 4. Example of determination of reaction order by fitting Eq. (4) to experimental data from temperature ramp test.

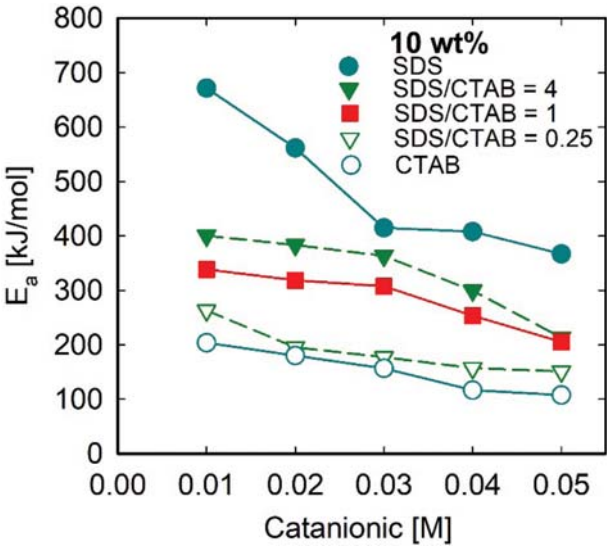

Fig. 5. Estimated activation energies of 10 wt% BSA as functions of catanionic surfactant concentrations.

Using 10 wt% BSA/catanionic solution as a reference point, best fit to Eq. (4) was obtained with n=1 (first-order) and R^2=0.99 (Fig. 4), indicating a first-order reaction. Thus, this reaction order matched well our kinetic findings during isothermal heating (discussed later).

Using the slope of Fig. 4, activation energies were calculated for 10 wt% BSA/catanionic gels with various SDS/CTAB mixing ratio. Gelation activation energies were quite different for BSA/catanionic solutions with different SDS/CTAB mixing ratio. Fig. 5 shows estimated activation energies as functions of catanionic surfactant concentration. The figure shows that the lower activation energy of cationic-rich solutions is in-line with the higher gelation rate of the solutions during non-isothermal heating, indicating CTAB-rich solutions increased the gelation rate of BSA by lowering the activation energy of gelation. Furthermore, the activation energy was found to be concentration dependent [45,46] and to decrease with

increasing catanionic surfactant concentration. This finding agrees well with that of Silva et al. [46] who found the activation energy of solvent induced-lysozyme gelation decreased as concentration of tetramethylurea increased.

4. Isothermal Gelation of BSA/Catanionic Solutions

Isothermal gelation of BSA/catanionic solutions was more rapid than the non-isothermal gelation due to the high constant heating temperature. In the case of anionic-rich solutions with SDS/CTAB= 4.0 (discussed later) the gelation rate (i.e., the inverse of t_{gel}) was much lower than those of cationic-rich solutions, and in order to observe the t_{gel} a higher isothermal heating temperature was used. That is, BSA/catanionic solutions with SDS/CTAB=4.0 were heated isothermally at 90 °C, while BSA/catanionic solutions with SDS/CTAB= 1.0 and 0.25 were heated isothermally at 80 and 70 °C, respectively. A typical gelation process of BSA/catanionic solution is shown in Fig. 6 below and the rest of the gelation curves are shown in supporting information Figs. S4-S6. The evolution of storage modulus (G′), loss modulus (G″), and tan δ were plotted as functions of the heating time to describe the gelation of 10 wt% BSA in 0.05 M of catanionic surfactant with SDS/CTAB=1.0. At the early stage ($t<t_{gel}$), G′ and G″ increased slowly with time, while tan δ decreased rapidly. This was attributed to heat-induced denaturation of the BSA (just like the case of non-isothermal gelation), since protein unfolding is marked by gradual increase in solution viscosity [1,47, 48]. After a certain period of induction time (t_{gel}), G′ and G″ started to increase abruptly, suggesting the denatured and unfolded protein chains which exposed the initially buried hydrophobic core were forming aggregates and gel. At the late stage, G′ and G″ increased steadily and hardly reached the saturated values. However, the increase in G′ and G″ after reaching a plateau value was slower than that at the onset of gelation, which suggested that the kinetics at onset of gelation was faster than that beyond the plateau storage modulus. Meanwhile, tan δ appeared to level off, which described a stage where the gel network further developed from a soft gel to a hard gel state [49-51].

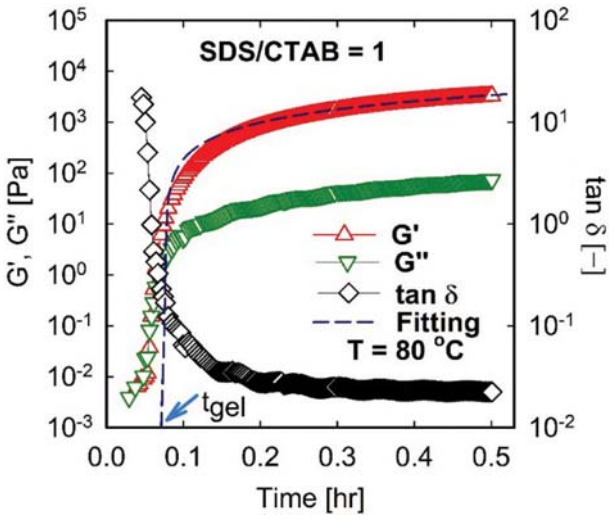

Fig. 6. Time sweep test for 10 wt% BSA solution in 0.05 M catanionic surfactant, with frequency of ω=1 rad/s, strain amplitude γ=0.05, SDS/CTAB=1.

The gel time of the reaction during isothermal heating, which is illustrated in Fig. 6 (pointed towards with arrow) is closely related to rheological properties. It indicates the beginning of crosslinking or network formation, where the protein changes from liquid state to a solid/gel state. The gel time can be determined according to different criteria [49], such as the base line and the tangent drawn from the turning point of G′ [24], or the time where tan δ equals 1, or G′ and G″ curves crossover [50]. Grisel and Muller [26] used the point where tan δ is independent of frequency, which is also known as the Winter-Chambon criterion to determine the gel time for Schizophyllan (SPG)-Borax systems. However, a later study found that values of tan δ at various frequencies have no one-pointed crossover during gelation of SPG-Borax [51]. Moreover, Fang et al. [51] stressed that the Winter-Chambon criterion is not powerful in determining the critical gelation point of some rapidly gelling systems. Therefore, it would appear that the method to be employed for accurate t_{gel} determination is system dependent [49].

In the present study, it was difficult to detect the t_{gel} by the crossover of G′ and G″ curves because the strong attraction between oppositely charged cationic and anionic surfactants made the formation of catanionic surfactant mixed aggregates favorable at the solution state (i.e. G′≡G″ or >G″ prior to t_{gel} for all the SDS/CTAB mixing ratio examined). Therefore we sought for a more accurate model that could describe the growth of the BSA/catanionic gel network under isothermal heating.

Since the non-isothermal gelation showed a first-order reaction, we applied the same reaction order to model the isothermal gelation. Moreover the first-order kinetic model has been used extensively to fit the isothermal gelation processes of biopolymers such as glycinin [52], β-conglycinin [52], casein [53], konjac glucomannan [54] and Schizophyllan [51]. The first-order kinetic model can be written as follows:

$$G'(t)=G'_{sat}[1-\exp(-(t-t_{gel})/\tau_c)] \quad (5)$$

Where t_{gel} is gel time, τ_c is a characteristic time, the reciprocal of which reflects the gelation rate, and G'_{sat} is the saturated storage modulus after infinitely long time. It should be noted that by curve fitting, we can obtain the saturated value of G′ which can never be achieved in actual observation. The kinetic parameters estimated by curve fitting for 10 wt% BSA in catanionic solutions with various SDS/CTAB mixing ratio are shown in Figs. 7 and 8, while the fitting of equation 5 to G′ curves is shown in supporting information Fig. S4(f).

The use of a first-order kinetic modeling for protein gelation can be understood this way: Tobitani and Ross-Murphy [55] proposed that protein gelation kinetics proceeded in multi-steps with different reaction rates. They suggested four distinct steps which can be assumed as follows:

$$\begin{aligned} &P \xrightarrow{k_1} U && \text{unfolding of native proteins}\\ &U+U \xrightarrow{k_2} A && \text{aggregation of unfolded proteins}\\ &A+A \underset{k_{a2}}{\rightleftharpoons} R && \text{intermolecular reaction of aggregates}\\ &R \underset{k_f}{\rightleftharpoons} R' && \text{intramolecular reaction of aggregates} \end{aligned} \quad (6)$$

Shakhnovich and Finkelstein [16] observed that the protein unfold-

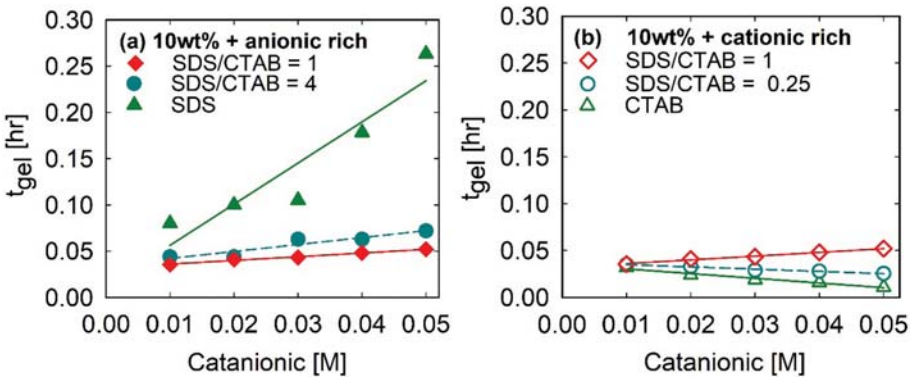

Fig. 7. Gel time for 10 wt% BSA as a function of various catanionic concentration (a) anionic rich solution (b) cationic rich solution.

ing step is first-order in protein concentration, and further stressed that the cornerstone of protein denaturation is the disruption of tight packing of the side chains in the protein core, which is independent of the protein-solvent interactions. However, it is generally accepted that the second and the third reaction steps (intermolecular aggregation steps) are second-order reactions [55]. Comparatively the protein unfolding step is the fastest in terms of reaction rates. The intermolecular and intramolecular reaction steps are governed by non-covalent bonding and can be regarded as reversible reactions [55]. Since the establishment of the equilibrium for the intermolecular reaction of aggregates is appreciably faster than that of the intramolecular reaction aggregates the latter one is the rate determining step. In this situation, the overall kinetics is approximately first-order in protein concentration. Moreover, following conventional reaction kinetics, the intramolecular reaction step in Eq. (6) is of one lower order (first-order in protein concentration) compared to the corresponding intermolecular steps. Therefore, it is reasonable that the isothermal gelation process is well fitted by first-order kinetic model (Eq. (5)).

5. Effects of Catanionic Concentration and SDS/CATB Mixing Ratio on t_{gel}, τ_c and G_{sat} of BSA

The effects of increasing the catanionic concentration and the SDS/CTAB mixing ratio on the t_{gel}, τ_c and G'_{sat} of BSA were investigated. It can be seen in Fig. 7 that the lowest gelation rate (or the highest t_{gel}) was observed for anionic-rich solutions with SDS/CTAB=4.0, while highest gelation rate was observed for cationic-rich region with SDS/CTAB=0.25. Equal molar ratio of SDS and CTAB (i.e., SDS/CTAB=1.0) showed a gel time in the halfway between the anionic and cationic-rich regions.

The underlying source of higher rate of denaturation and gelation of BSA in cationic-rich solutions is connected with the interaction mode of the CTAB polar head group with charged protein residues. These interactions can be rationalized as follows: The isoelectric point (IEP) of BSA is at pH 4.5-5.0, which implies that the protein is negatively charged at neutral pH [56,57], and the positively charged CTAB head group (CTA^+) would interact more strongly with the protein by electrostatic attraction, while the CTAB hydrophobic tail group binds with the BSA by hydrophobic interaction, operating cooperatively to favor the denaturation process [4]. These non-native binding interactions of CTAB with the protein residues destabilized the native non-covalent interactions that stabilized the protein and hence caused unfolding of the protein, which resulted in faster gelation of BSA in cationic-rich solutions. In the case of anionic rich solutions (i.e., SDS/CTAB=4.0), the denaturing power of SDS on BSA was weakened by electrostatic repulsion between SDS head group and some BSA side chains bearing similar charge. Such electrostatic repulsion that weakens the denaturing effect of SDS on a negatively charged protein at neutral pH has been reported previously [58]. For instance, Jonsson and Johansson [58] observed that at low ionic strength, a cationic hydrophobically modified ethylene oxide polymer (HM-EO) attracted negatively charged BSA and repelled positively charged lysozyme, while upon addition of SDS the negatively charged aggregates attracted lysozyme and repelled BSA. However, in the case of equimolarly mixed catanionic solutions (i.e., SDS/CTAB=1.0), the very strong attraction between oppositely charged cationic and anionic surfactants head groups caused the formation of catanionic surfactant mixed aggregates in the bulk solution a more favorable process than binding to the protein. For this reason, the faster rate of BSA denaturation and gelation evident in the cationic-rich solutions (SDS/CTAB=0.25), was reduced in equimolarly mixed catanionic solutions and thereby caused the t_{gel} to increase.

Furthermore, the t_{gel} decreased with increasing catanionic concentration for cationic-rich solutions (SDS/CTAB=0.25), while for anionic-rich and equimolarly mixed surfactants (SDS/CTAB=4.0 and 1.0), increase in catanionic concentration increased the t_{gel}. This interesting phenomenon has been described as the protective effect of SDS against thermal denaturation of proteins [9,59-62]. Moriyama et al. [59] studied secondary structural change in bovine serum albumin at temperatures up to 130 °C and the protective effect of SDS using circular dichroism. They observed that the helical content lost by the BSA during thermal denaturation was recovered upon addition of SDS. According to the authors, the SDS protective effect was found to be caused by a cross-linking function of the SDS ion between a group of non-polar residues and a positively charged residue in the protein. Similarly, SDS has been reported to protect ovalbumin [60] and human serum albumin [62] from thermal denaturation. Therefore, due to the recovery of BSA helicity in equimolarly mixed and anionic-rich solutions, the t_{gel} increased with catanionic surfactant concentration at the temperature range examined. Note that the SDS protective effect was less dominant during non-isothermal heating because temperature increased at a slow

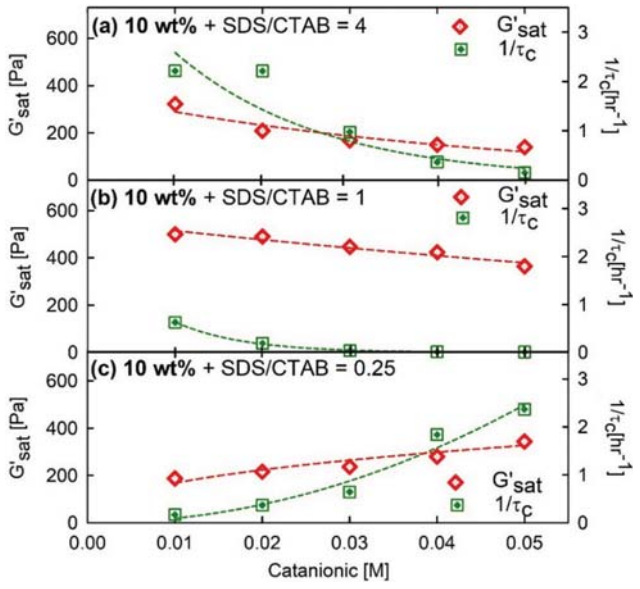

Fig. 8. Saturated storage modulus (G'_{sat}) and reaction rate ($1/\tau_c$) for 10 wt% BSA as a function of catanionic concentration (a) anionic rich solution (b) equimolarly mixed solution (c) cationic rich solution.

rate (0.5 °C/min), suggesting the stability of BSA was affected predominantly by denaturants in solution. Therefore, the SDS driven denaturation appeared to offset its protective effect during non-isothermal heating and for this reason, the T_{gel} decreased with increasing catanionic concentration for anionic-rich and equimolarly mixed solutions (i.e. SDS/CTAB=4.0 and 1.0, Figs. 2(b) and 3).

Fig. 8 shows the variation of G'_{sat} and $1/\tau_c$ with catanionic concentration. Obviously, the saturated storage modulus increased with catanionic concentration with SDS/CTAB=0.25 but decreased with increase in catanionic concentration with SDS/CTAB=4.0 and 1.0, which is consistent with the trend observed for the t_{gel}. Additionally, the gelation rate, $1/\tau_c$, increased with increasing catanionic concentration with SDS/CTAB=0.25 which also agrees well with the t_{gel}. The saturated storage modulus is directly related to the strength of the BSA/catanionic gel and the degree of cross-linking. Therefore our finding suggests that the gel rigidity and the rate of gelation can be optimized by varying SDS/CTAB mixing ratio at a given BSA concentration and isothermal heating temperature.

6. Effect of BSA Concentration on t_{gel}, τ_c and G_{sat} of BSA

The effect of BSA concentration was investigated using concentrations of 5 and 7 wt% in addition to 10 wt% (discussed above) and catanionic surfactant concentrations of 0.0-0.05 M. The G′ spectrum of curves as a function of heating time is shown in supporting information Fig. S5 for 7 wt% and Fig. S6 for 5 wt%. In the BSA concentration range examined, the G′ was found to increase continuously but subtly after reaching a plateau value, contributing to further strengthening of the gel network, which is an indication that BSA/catanionic gels are thermally irreversible. The G′ of a gel is considered to be proportional to the number of elastically active network chains (EANCs) in the gel-per-unit volume or to be inversely proportional to the chain molecular weight M_c between crosslinks in gel network [53]. Moreover the nature of bonds in the gel which is dominated by electrostatic and hydrophobic interactions may also affect the values of G′. On the basis of this assumption, we found that increasing the BSA concentration from 5 to 7 wt% resulted in more elastically active network chains-per-unit volume or a smaller chain molecular weight between crosslinks in the gel network. This was attributed to the more protein-protein interactions on increasing BSA concentration [1,53]. In addition, the G′ spectra of curves for 5 wt% BSA solutions showed initial structure development started at longer heating times due to lower protein-protein interactions when compared with 7 wt% BSA solu-

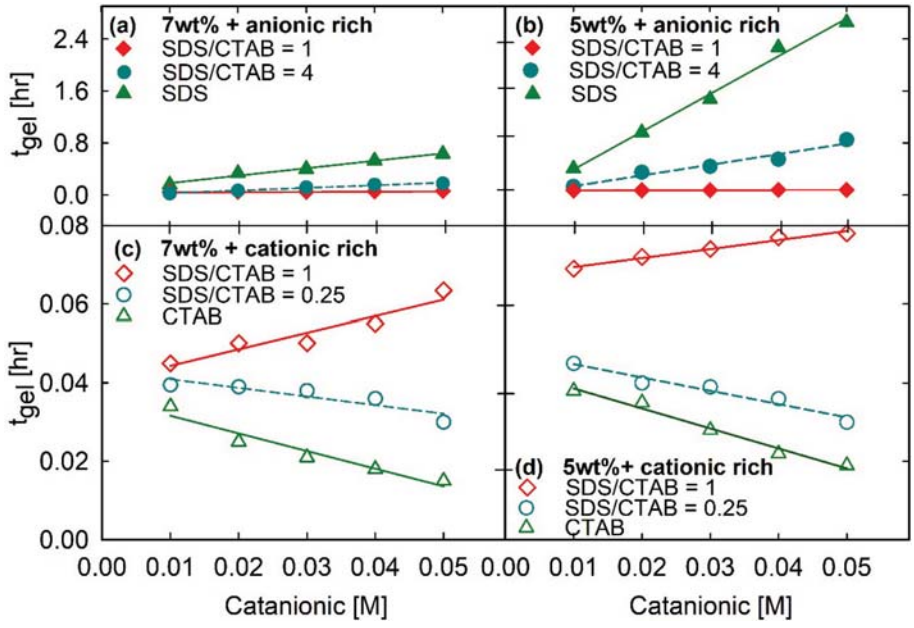

Fig. 9. (a)-(d) Gel time for 5 and 7 wt% BSA as a function of various catanionic concentration with various SDS/CTAB mixing ratios.

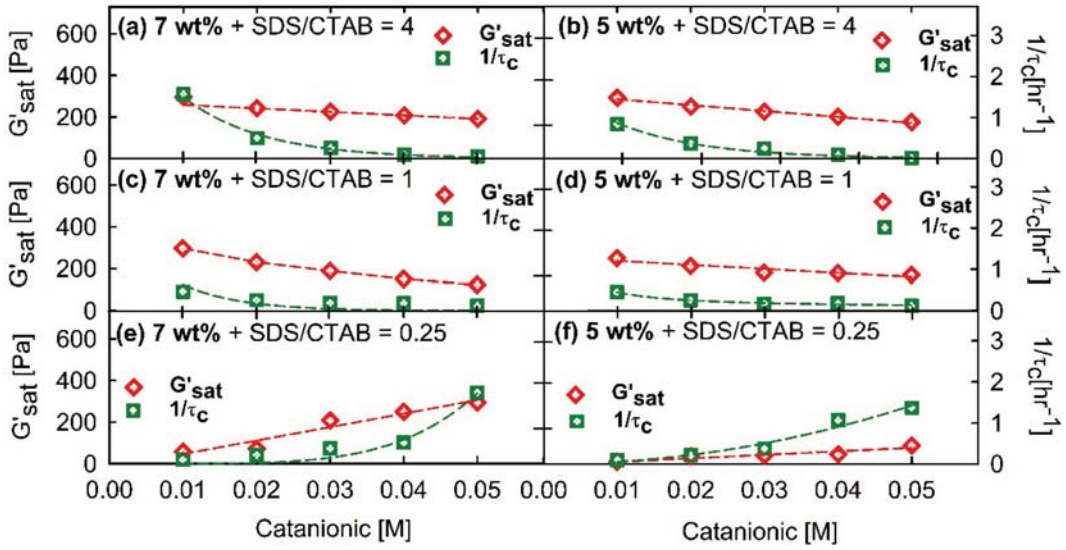

Fig. 10. (a)-(f) Saturated storage modulus (G'_{sat}) versus reaction rate ($1/\tau_c$) for 5 and 7 wt% BSA as a function of various catanionic concentration with various SDS/CTAB mixing ratio.

tions. It should be recalled that different isothermal heating temperatures were used for each of the SDS/CTAB mixing ratio and for this reason only 5 and 7 wt% BSA concentration with the same SDS/CTAB mixing ratio can be compared directly. Fig. 9(a)-(d) shows the variation of t_{gel} with catanionic surfactant concentration for 5 and 7 wt% BSA. For anionic-rich solutions, t_{gel} was found to decrease significantly with increase in BSA concentration throughout the surfactant concentration ranges examined, which indicated that there was a lag period before the commencement of gelation of the 5 wt% BSA solutions when compared with 7 wt%. In the case of cationic-rich solutions, the t_{gel} did not vary significantly with BSA concentration, especially for BSA solutions with SDS/CTAB=0.25 (Fig. 9). Fig. 10(a)-(f) shows the plots of G'_{sat} and $1/\tau_c$ versus catanionic concentration for 5 and 7 wt% BSA. Judging by the G'_{sat} values predicted by first-order reaction kinetic model (supporting information Figs. S6(f) and S5(f)), the gel stiffness and degree of cross-linking increased with BSA concentration for a given catanionic concentration with SDS/CTAB mixing ratio of 0.25 and 1 (Fig. 10). Anionic-rich solutions (SDS/CTAB=4.0) showed very close values of G'_{sat} presumably because the 5 wt% solutions were heated for a longer period (supporting information Fig. S6(c)). The rate of reaction ($1/\tau_c$) and saturated storage modulus (G'_{sat}) showed direct relationship with catanionic surfactant concentration for 5 and 7 wt% BSA with SDS/CTAB=0.25. However for 5 and 7 wt% BSA with SDS/CTAB=1.0 and 4.0, the tendency of SDS to recover the protein helicity or to protect it against thermal denaturation was amplified over denaturation and gelation, which caused G'_{sat} and $1/\tau_c$ to decrease with increasing catanionic concentration (Fig. 10(a)-(f)).

CONCLUSIONS

The effects of catanionic surfactant consisting of various SDS/CTAB mixing ratio on the gelation kinetics of bovine serum albumin (BSA) were investigated under isothermal and non-isothermal conditions.

Under non-isothermal condition, increasing the BSA or catanionic concentration decreased the T_{gel} irrespective of the SDS/CTAB mixing ratio. A non-isothermal kinetic model which combines reaction rate and Arrhenius type relationship was found to describe well the non-isothermal gelation of the BSA/catanionic solutions. Gelation activation energies estimated using non-isothermal kinetic model were quite different for BSA/catanionic solutions with various SDS/CTAB mixing ratio. The activation energy was lower for cationic-rich solutions than anionic-rich solutions, which indicated that it was energetically more favorable for BSA/cationic-rich solutions to gel than the BSA/anionic-rich solutions. In addition, the activation energy was found to be concentration dependent, and to decrease with increasing catanionic surfactant concentration. The reaction order determined by non-isothermal kinetics is first-order and matched well our kinetic findings during isothermal heating.

For isothermal heating, BSA with anionic-rich solutions and equimolarly mixed surfactants had slower gelation rates (or higher t_{gel}) than BSA with cationic-rich solutions, which agreed well with non-isothermal gelation. Interestingly, increasing catanionic surfactant concentration increased the t_{gel} of BSA with anionic-rich and equimolarly mixed surfactant solutions, while a decrease was observed for BSA with cationic-rich solutions. This phenomenon is described as a stabilizing effect of SDS against thermal denaturation and gelation of BSA under isothermal heating. Consequently the G'_{sat} (saturated storage modulus at infinite time) increased with catanionic concentration for cationic-rich solutions, but decreased with increasing catanionic concentration for anionic-rich solutions and equimolarly mixed solutions. The rate of gelation increased with increase in BSA concentration due to more protein-protein interaction at high BSA concentration. Under isothermal conditions, first-order reaction kinetics well described the kinetics of gel formation which agreed well with previous studies on heat-induced biopolymer gels.

Overall, these findings present detailed features of catanionic

surfactant mixtures and their interaction with protein. The kinetic parameters provide better ways of modelling protein gelation, while the stabilizing and denaturing effects of the catanionic mixtures are advantageous for studies on solvent-induced protein stability and protein folding.

ACKNOWLEDGEMENTS

This study was supported by the Basic Science Research Program (2018R1D1A1B07050934) through the National Research Foundation of Korea (NRF).

SUPPORTING INFORMATION

Additional information as noted in the text. This information is available via the Internet at http://www.springer.com/chemistry/journal/11814.

REFERENCES

1. O. S. Nnyigide, Y. Oh, H. Song, E. Park, S. Choi and K. Hyun, *Korea-Aust. Rheol. J.*, **29**, 101 (2017).
2. Z. Yu, M. Yu, Z. Zhang, G. Hong and Q. Xiong, *Nanoscale Res. Lett.*, **9**, 343 (2014).
3. A. Chakraborty and S. Basak, *Colloids Surf., B*, **63**, 83 (2008).
4. A. Rogozea, I. Matei, I. Turcu, G. Ionita, V. Sahini and A. Salifoglou, *J. Phys. Chem. B*, **116**, 14245 (2012).
5. G. Wang, H. Hou, Y. Chen, C. Yan, G. Baiab and Y. Luab, *RSC Adv.*, **6**, 19700 (2016).
6. Z. Wasylewski and A. Kozik, *Eur. J. Biochem.*, **95**, 121 (1979).
7. W. Sukow, H. Sandberg, E. Lewis, D. Eatough and L. Hansen, *Biochemistry*, **19**, 912 (1980).
8. M. Bolattin, S. Nandibewoor, S. Joshi, S. Dixit and S. Chimatadar, *RSC Adv.*, **6**, 63463 (2016).
9. R. B. Singh, S. Mahanta and N. Guchhait, *Chem. Phys. Lett.*, **463**, 183 (2008).
10. L. R. Arriaga, D. Varade, D. Carriere, W. Drenckhan and D. Langevin, *Langmuir*, **29**, 3214 (2013).
11. R. Lu, N. Cao, L. Lai, B. Zhu, G. Zhao and J. Xiao, *Colloids Surf., B*, **41**, 139 (2005).
12. A. Renoncourt, *Study of supra-aggregates in catanionic surfactant systems*, Doctoral Dissertation, Institute of Physical and Theoretical Chemistry, University of Regensburg (2005).
13. L. Donato, C. Garnier, B. Novales, S. Durand and J. Doublier, *Biomacromolecules*, **6**, 374 (2005).
14. L. Bocker, P. A. Ruhs, L. Boni, P. Fischer and S. Kuster, *ACS Biomater. Sci. Eng.*, **2**, 90 (2016).
15. J. K. Gillham and J. A. Benci, *J. Appl. Polym. Sci.*, **18**, 951 (1974).
16. E. I. Shakhnovich and A. V. Finkelstein, *Biopolymers*, **28**, 1667 (1989).
17. J. Ahmed, H. S. Ramaswamy and I. Alli, *J. Food Sci.*, **71**, 158 (2006).
18. H. Singh and A. Waungana, *Int. Dairy J.*, **11**, 543 (2001).
19. M. M. O. Eleya and S. Gunasekaran, *J. Food Sci.*, **67**, 725 (2002).
20. P. Date and D. Ottoor, *Polym. Plast. Technol. Eng.*, **55**, 403 (2016).
21. S. Salzer, N. A. Rosema, E. C. Martin, D. E. Slot, C. J. Timmer, C. E. Dorfer and G. A. van der Weijden, *Clin. Oral Invest.*, **20**, 443 (2016).
22. A. Patel, K. Cholkar and A. K. Mitra, *Ther. Deliv.*, **5**, 337 (2014).
23. F. Chambon and H. H. Winter, *J. Rheol.*, **31**, 683 (1987).
24. J. Ampudia, E. Larrauri, E. M. Gil, M. Rodriguez and L. M. Leon, *J. Appl. Polym. Sci.*, **71**, 1239 (1997).
25. J. M. Laza, C. A. Julian, E. Larrauri, M. Rodriguez and L. M. Leon, *Polymer*, **40**, 35 (1998).
26. M. Grisel and G. Muller, *Macromolecules*, **31**, 4277 (1998).
27. S. A. Madbouly and J. U. Otaigbe, *Macromolecules*, **39**, 4144 (2006).
28. S. De Maria, G. Ferrari and P. Maresca, *Food Nutr. Sci.*, **6**, 770 (2015).
29. K. Hyun, M. Wilhelm, C. O. Klein, K. S. Cho, J. G. Nam, K. H. Ahn, S. J. Lee, R. H. Ewoldt and G. H. McKinley, *Prog. Polym. Sci.*, **36**, 1697 (2011).
30. I. S. Chronakis, *J. Agric. Food Chem.*, **49**, 888 (2001).
31. F. S. M Van Kleef, *Biopolymers*, **25**, 31 (1986).
32. M. D. Alvarez, F. J. Cuesta, B. Herranz and W. Canet, *Foods*, **6**, 3 (2017).
33. D. E. Otzen, *Biophys. J.*, **83**, 2219 (2002).
34. A. Valstar, Protein-Surfactant Interactions, Ph.D. Dissertations, Uppsala University, Uppsala, Sweden (2000).
35. M. C. Puppo and M. C. Anon, *J. Agric. Food Chem.*, **46**, 3039 (1998).
36. M. Yoshida, K. Kohyama and K. Nishinari, *Biosci. Biotechnol. Biochem.*, **56**, 725 (1992).
37. C. L. Bon, T. Nicolai and D. Durand, *Macromolecules*, **32**, 6120 (1999).
38. O. S. Nnyigide and K. Hyun, *J. Chem. Technol. Metall.*, **51**, 147 (2016).
39. M. Migliori, D. Gabriele, N. Baldino, F. R. Lupi and B. De Cindio, *J. Food Proc. Eng.*, **34**, 1266 (2011).
40. H. H. Chen, H. Y. Kang and S. D. Chen, *J. Food Eng.*, **88**, 45 (2008).
41. M. D. Alvarez, R. Fuentes, M. D. Olivares, F. J. Cuesta and W. Canet, *J. Food Eng.*, **136**, 9 (2014).
42. J. W. Rhim, R. V. Nunes, V. A. Jones and K. R. Swartzel, *J. Food Sci.*, **54**, 446 (1989).
43. J. Ahmed, H. S. Ramaswamy, A. Ayad and I. Alli, *Food Hydrocoll.*, **22**, 278 (2008).
44. J. A. Da Silva, M. P. Gongalves and M. A. Rao, *Int. J. Biol. Macromol.*, **17**, 25 (1995).
45. W. B. Yoon, S. Gunasekaran and J. W. Park, *J. Food Sci.*, **69**, E238 (2004).
46. M. A. Da Silva and E. P. Areas, *J. Colloid Interface Sci.*, **289**, 394 (2005).
47. S. Kundu, A. J. Chinchalikar, K. Das, V. K. Aswal and J. Kohlbrecher, *Chem. Phys. Lett.*, **584**, 172 (2013).
48. F. Lefevre, B. Fauconneau, A. Ouali and J. Culioli, *J. Sci. Food Agric.*, **82**, 452 (2002).
49. L. Sun, Thermal Rheological Analysis of Cure Process of Epoxy Prepreg, Doctoral Dissertation, The Department of Chemical Engineering, Louisiana State University (2002).
50. C. Y. M. Tung and P. J. Dynes, *J. Appl. Poly. Sci.*, **27**, 569 (1982).
51. Y. Fang, R. Takahashi and K. Nishinari, *Biomacromolecules*, **5**, 126 (2004).
52. K. Kohyama and K. Nishinari, *J. Agric. Food Chem.*, **41**, 8 (1993).
53. R. Niki, K. Kohyama, Y. Sano and K. Nishinari, *Polym. Gels Networks*, **2**, 105 (1994).
54. M. Yoshimura and K. Nishinari, *Food Hydrocolloids*, **13**, 227 (1999).

55. A. Tobitani and S. B. Ross-Murphy, *Macromolecules*, **30**, 4845 (1997).
56. B. Jachimska, M. Wasilewska and Z. Adamczyk, *Langmuir*, **24**, 6866 (2008).
57. O. S. Nnyigide, S. G. Lee and K. Hyun, *J. Mol. Model.*, **24**, 75 (2018).
58. M. Jonsson and H. Johansson, *J. Chromatogr. A*, **983**, 133 (2003).
59. Y. Moriyama, E. Watanabe, K. Kobayachi, H. Harano, E. Inui and K. Takeda, *J. Phys. Chem. B*, **112**, 16585 (2008).
60. J. C. Holt and J. M. Creeth, *Biochem. J.*, **129**, 665 (1972).
61. Y. Moriyama, Y. Sato and K. Takeda, *J. Colloid Interface Sci.*, **156**, 420 (1993).
62. G. Markus, R. L. Love and F. C. Wissler, *J. Biol. Chem.*, **239**, 3687 (1964).

Supporting Information

Rheo-kinetics of bovine serum albumin in catanionic surfactant systems

Osita Sunday Nnyigide and Kyu Hyun[†]

School of Chemical and Biomolecular Engineering, Pusan National University, Busan 46241, Korea
(*Received 28 May 2018 • accepted 18 July 2018*)

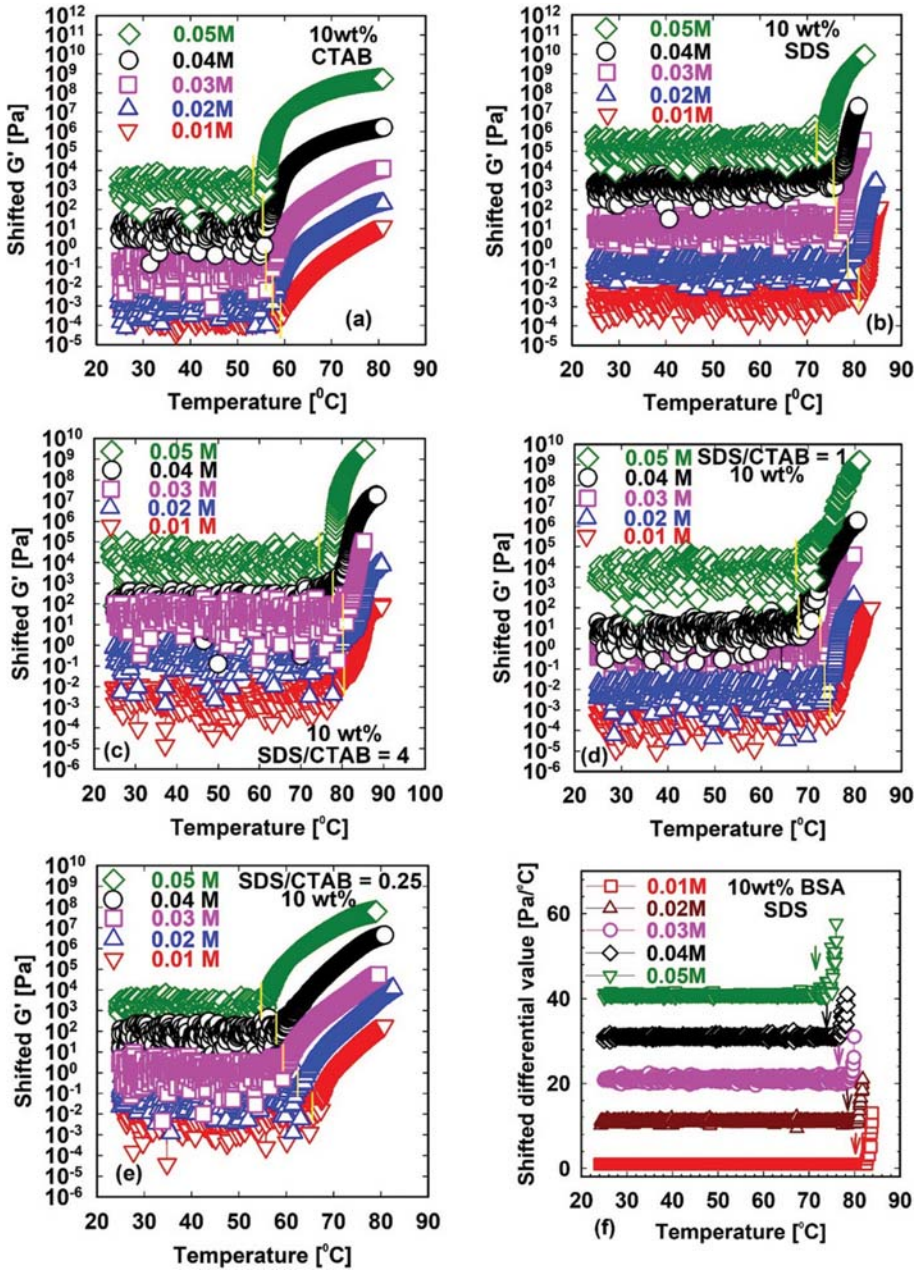

Fig. S1. Temperature ramp for 10 wt% BSA (a) CTAB (b) SDS (c) SDS/CTAB=4 (d) SDS/CTAB=1 (e) SDS/CTAB=0.25 and (f) example of determination of the gelation temperature for 10 wt% BSA in various SDS concentration using differential method. The yellow vertical lines in figure (a)-(e) were used subjectively to illustrate T_{gel}. Exact values were determined from the differential plot.

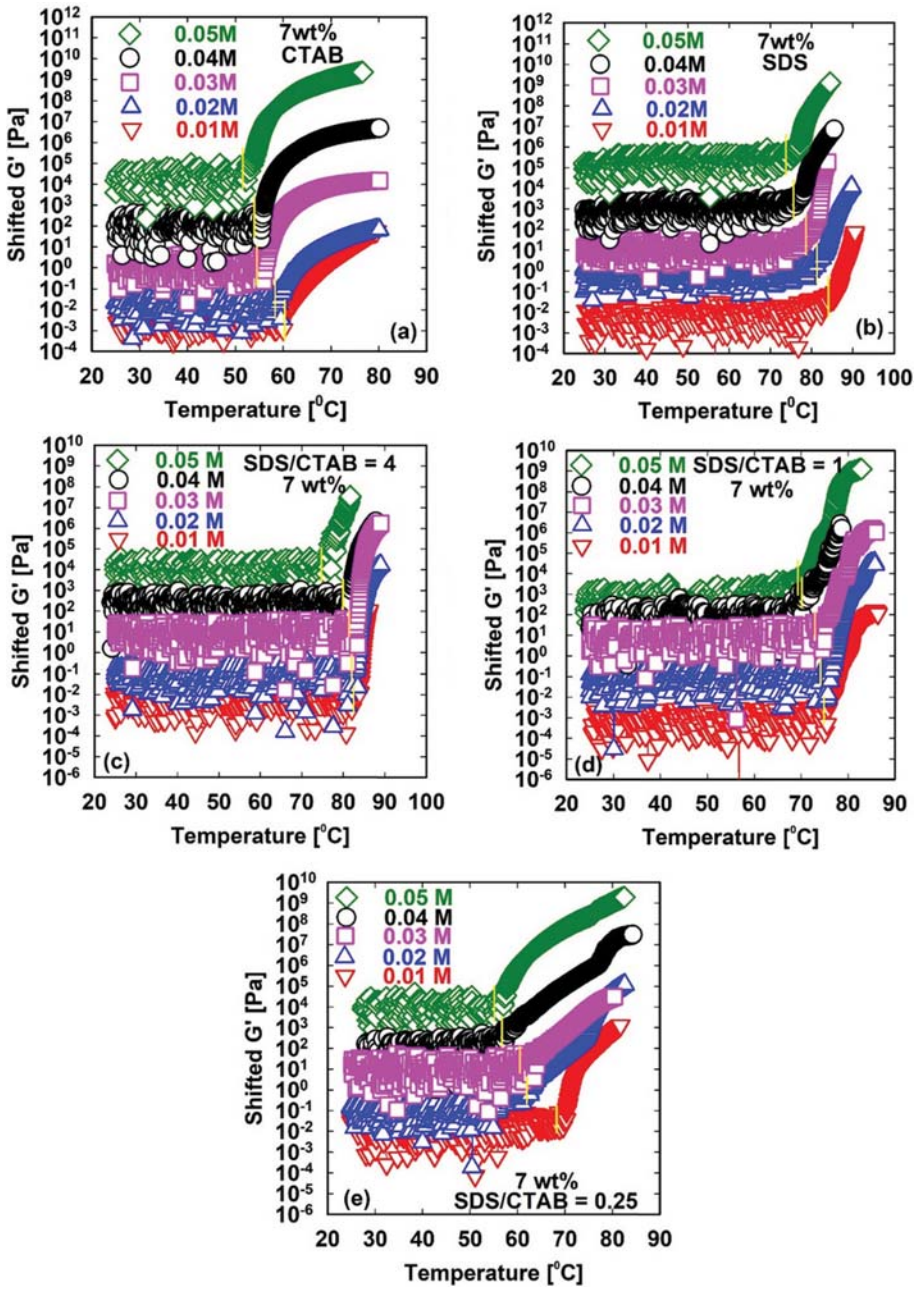

Fig. S2. Temperature ramp for 7 wt% BSA (a) CTAB (b) SDS (c) SDS/CTAB=4 (d) SDS/CTAB=1 and (e) SDS/CTAB=0.25.

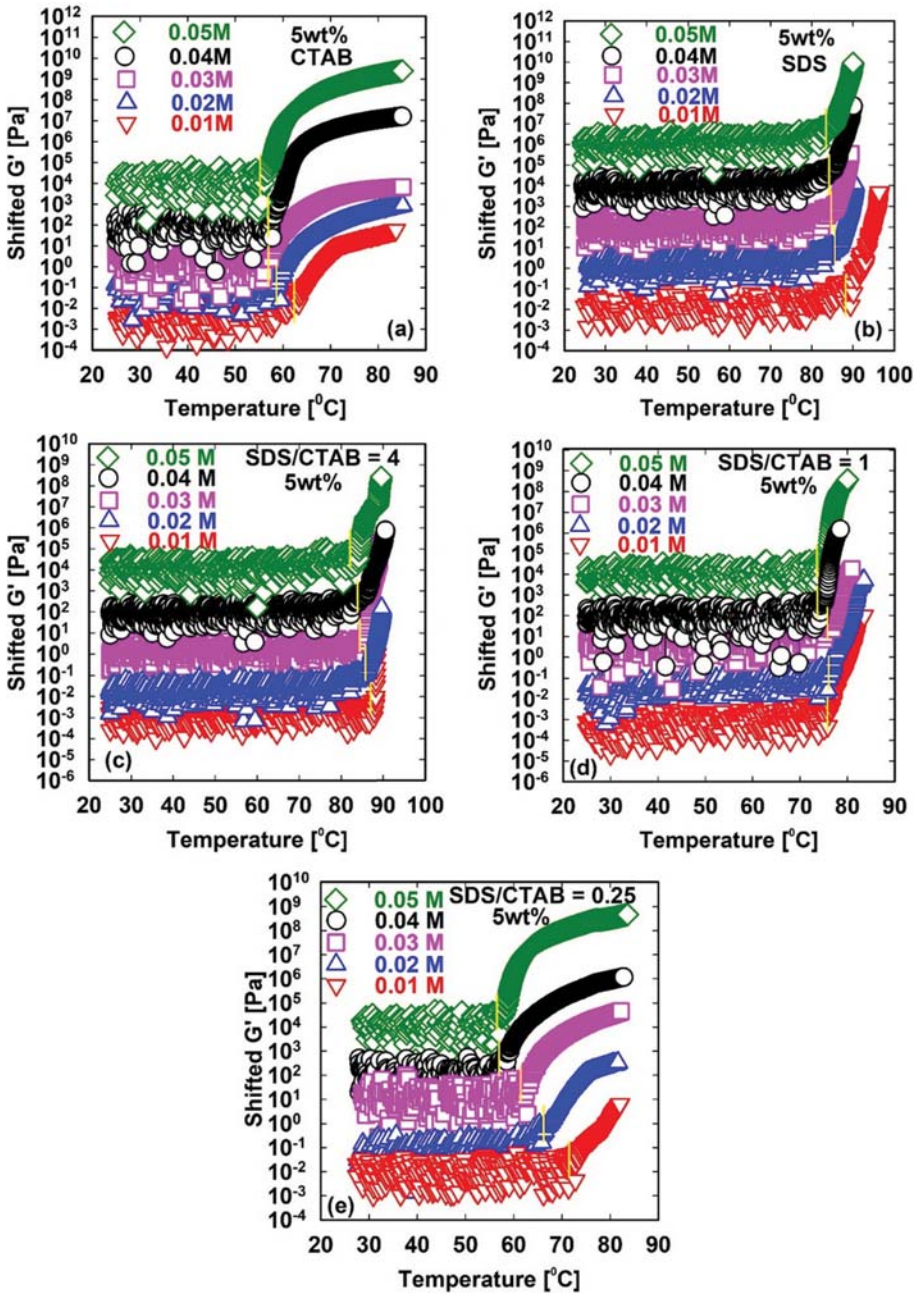

Fig. S3. Temperature ramp for 5 wt% BSA (a) CTAB (b) SDS (c) SDS/CTAB=4 (d) SDS/CTAB=1 and (e) SDS/CTAB=0.25.

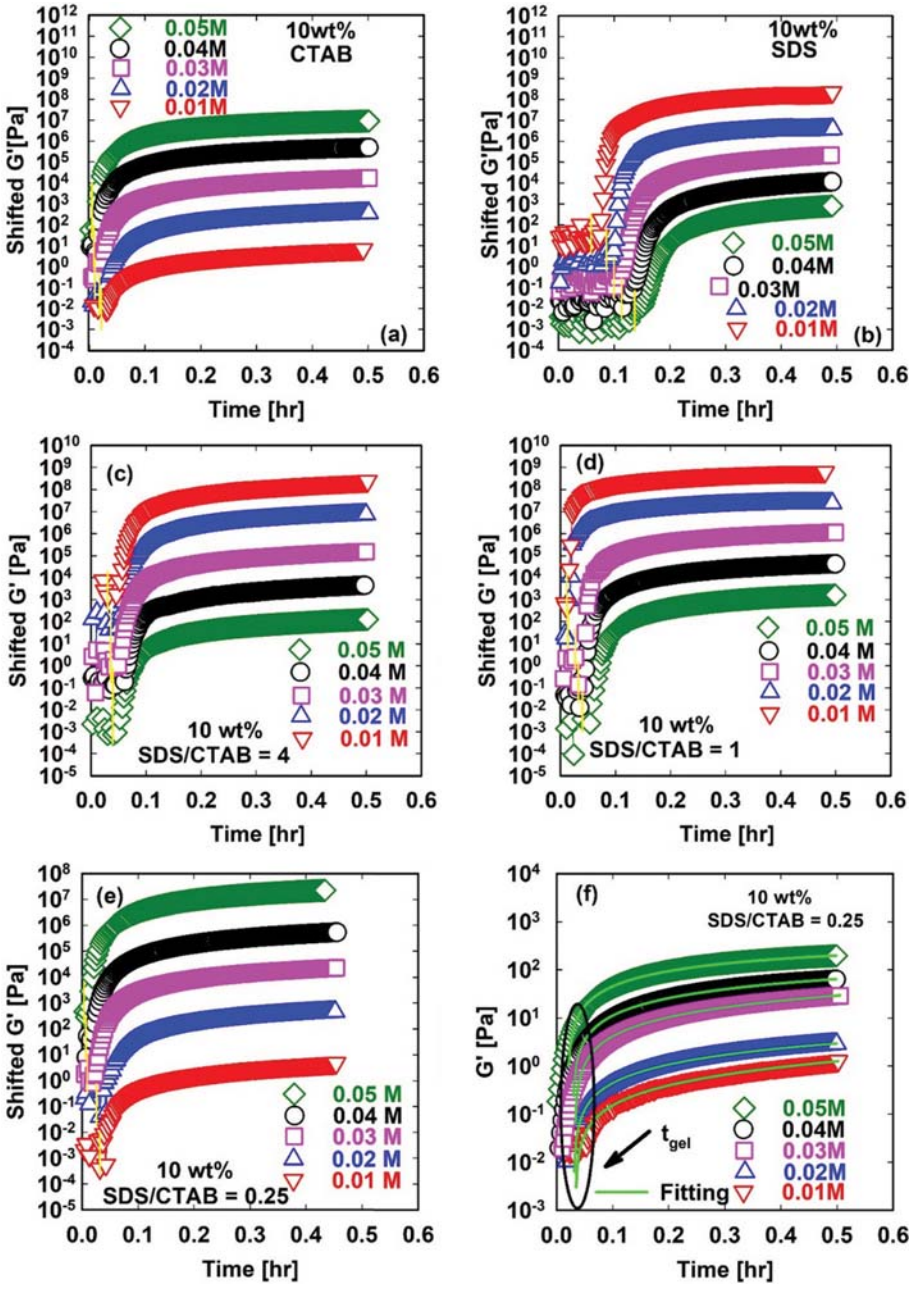

Fig. S4. Time sweep test for 10 wt% BSA (a) CTAB (b) SDS (c) SDS/CTAB=4 (d) SDS/CTAB=1 (e) SDS/CTAB=0.25 and (f) determination of gel time by fitting Eq. (5) to experiment data.

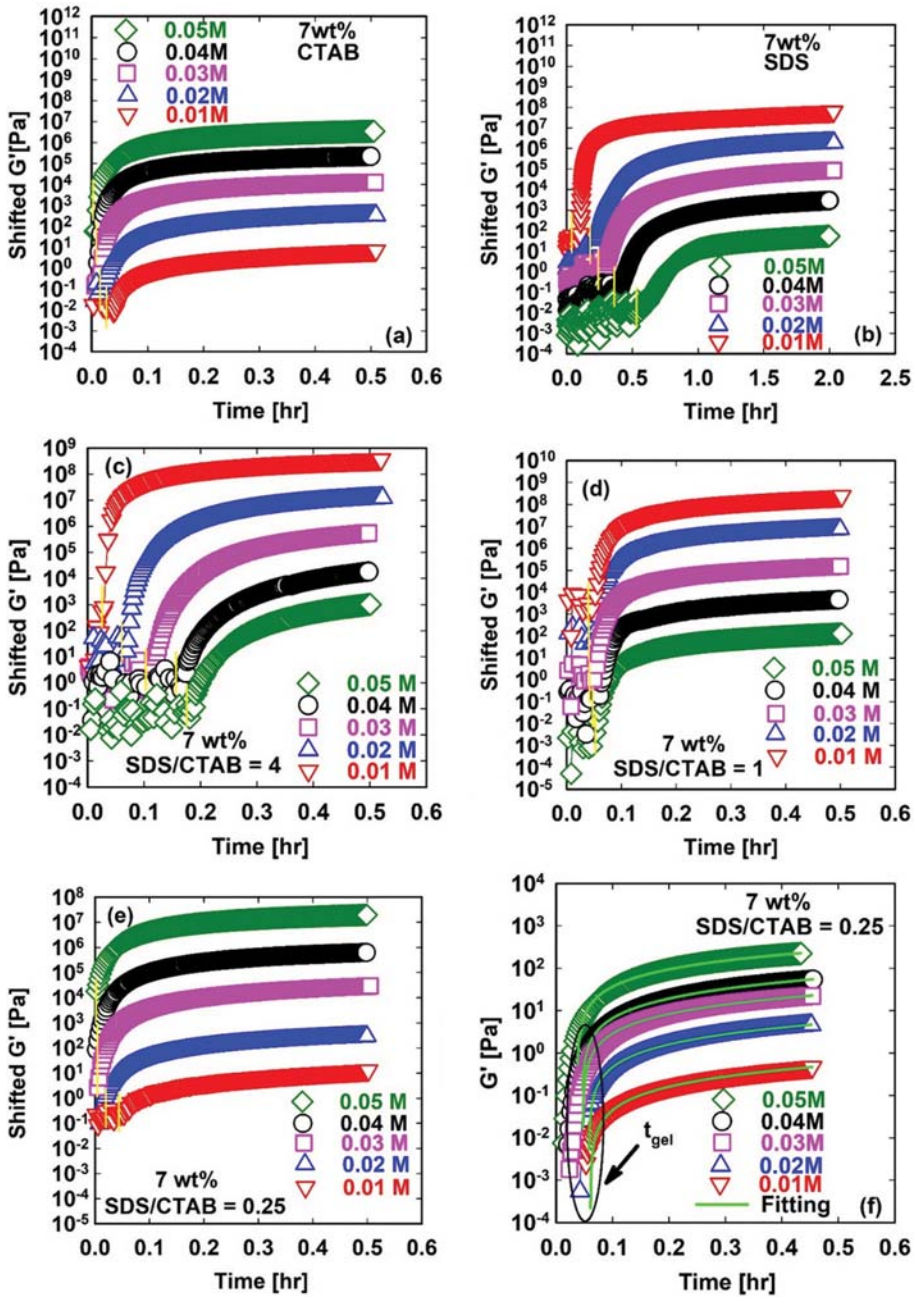

Fig. S5. Time sweep test for 7 wt% BSA (a) CTAB (b) SDS (c) SDS/CTAB=4 (d) SDS/CTAB=1 (e) SDS/CTAB=0.25 and (f) determination of gel time by fitting Eq. (5) to experiment data.

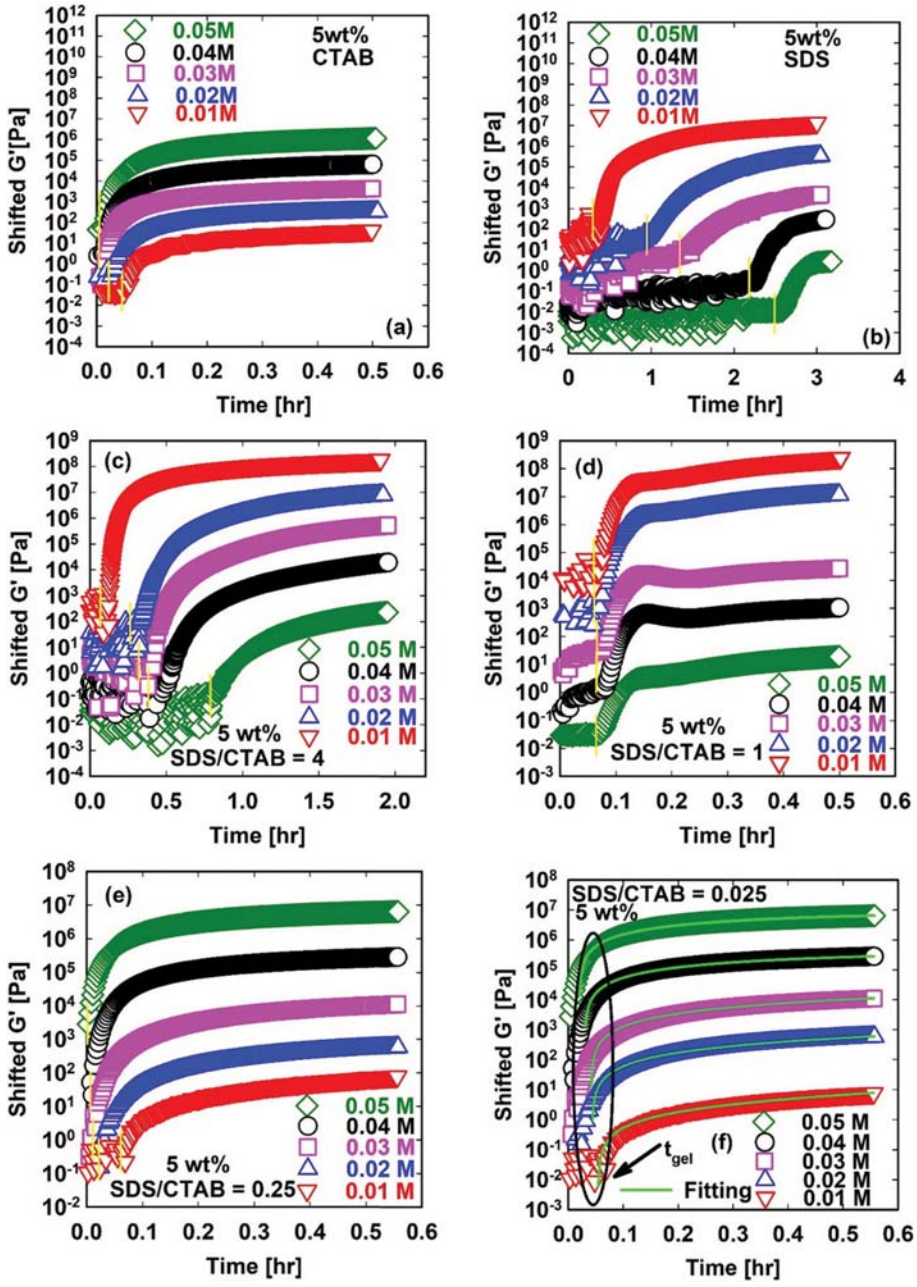

Fig. S6. Time sweep test for 5 wt% BSA (a) CTAB (b) SDS (c) SDS/CTAB=4 (d) SDS/CTAB=1 (e) SDS/CTAB=0.25 and (f) determination of gel time by fitting Eq. (5) to experiment data.